Numerical flow visualization of scale interactions at an internal boundary layer using streaklines

S. EMEIS

Institut für Meteorologie und Klimaforschung, Universität/Kernforschungszentrum Karlsruhe, Kaiserstrasse 12, *D*-7500 *Karlsruhe* 1, *F.R.G.*

Received June 16, 1988 ; revised November 11, 1988 ; accepted November 22, 1988

ABSTRACT. Streaklines computed with a numerical mesoscale model are used to show phenomena which occur at the interface of a boundary-layer behind a step and under a capping stable layer. Streaklines are a convenient method to trace the motion of fluid parcels and to indicate the regions of maximum vorticity in a streamflow.

By this means the formation of vortices at the interface can be analyzed. These vortices play an essential role for the entrainment of stable air from above through the interface.

Annales Geophysicae, 1989, **7,** (3), 213-220.

1. INTRODUCTION

Mesoscale numerical models have become a powerful tool to investigate atmospheric flow behaviour. These models today allow to perform more small-scale, more complex, and instationary simulations, but they also demand new and better ways to present the results. For stationary solutions one of the most common ways of presentation has been plots of streamlines. They showed both direction and strength of the flow. For instationary flows not only the state of the flow at the final time step is important but also the visualization of the development of the flow during the simulation.

In wind tunnel and water tank experiments flow structures and developments can be made visible by tracer substances advected with the fluid. Especially smoke in air flow studies and dye and gas bubbles in water flow studies are widely used. The numerical equivalent for the continuous injection of a tracer into a fluid at a fixed location is the streakline. A discontinuous injection leading to lines or bodies of dye or smoke in the fluid at certain instants can also be simulated in a numerical experiment. These features are referred to as material lines or material elements. An additional transport equation for passive tracer substances is necessary in the numerical model for this purpose.

In this paper streaklines and material elements shall be presented for the analysis of atmospheric flows. Streaklines have been used in the last few years to compare numerical simulations of vortex-shedding with visualization experiments in water channels (Perry *et al.*, 1982 ; Davis and Moore, 1982 ; Eaton, 1987). These studies showed that streaklines are a convenient method to display coherent structures in the flow as the formation and shedding of vorticies and to indicate vorticity in the flow.

Part 2 discusses different types of flow visualization and presents the numerical procedure for the streaklines. Part 3 gives a short introduction to the numerical model and the design of the numerical experiments and Part 4 gives the results of the visualization experiments.

2. FLOW VISUALIZATION

2.1. Streaklines

If flow computations are done with non-neutral stratification and non-homogeneous surface temperature, no stationary solution can be expected. Therefore the need for documentation of the instationary processes and developments is obvious.

There are different methods to show results of instationary flow simulations. Some of the most common are :

1) Contour plots of atmospheric variables present a « snap-shot » at a specified time step.

2) Streamlines are more suitable to display the flow direction, but only for a stationary flow field they are identical to the path of a particle through the model area.

3) Trajectories display the real path of a particle through the model area, but for instationary flow fields again no real flow patterns can be deduced from them. Only pathes of particles started at a fixed time step are visible.

In contrast to these methods streaklines are used here.

Streaklines give a continuous information on where particles originating from the same source are transported by the mean flow during the evolution of the flow field. Streaklines are suitable to follow eddies and other structures in the flow. They indicate where there is vorticity in the flow. The parameter that varies along a streakline is the residence time of the particles in the flow.

Streaklines indicate vorticity in two ways. In the case of vorticity due to curvature, that is where vortices are, the particles in the flow are attracted and forced to move around the vortex center. So the vortex is visible in the streakline plots by the collected particles in its center and the bending streaklines around its center. A deepening vortex collects more and more particles, a weekening one loses particles. No particles can enter in and no particles can leave from a stationary vortex.

But also pure shear vorticity is indicated by the streaklines by moving closer together. This can be understood from the following : consider a flow area between two horizontal lines z_1 and z_2 with $z_2 > z_1$. Let

$$\frac{\partial}{\partial z}\frac{\partial u}{\partial x} > 0 \quad \text{with} \quad \frac{\partial u}{\partial x}(z_1) = 0 .$$

This configuration can be found where shear is increasing with increasing x. From the equation of continuity it is then required that

$$\frac{\partial}{\partial z}\frac{\partial w}{\partial z} < 0 \quad \text{with} \quad \frac{\partial w}{\partial z}(z_1) = 0 .$$

This forces a vertical confluence $\left(\frac{\partial w}{\partial z} < 0\right)$ between z_1 and z_2. So a pair of streaklines entering a flow area of increasing shear vorticity will be brought closer together.

Due to these two mechanisms streaklines always tend to concentrate in areas of enhanced (positive or negative) vorticity in the flow. Davis and Moore (1982) proved this by an overlay of streakline plots on isovorticity plots.

Streaklines are produced by the following steps :

1) Insert particles at the time step from when on streaklines shall be produced.

2) Move particles one time step by the mean wind.

3) Insert new particles at the old origin.

4) Repeat from 2.

This is done by a transport equation for a passive tracer substance which is added to the mesoscale numerical model. Passive means that the tracer particles have no effect back on the mean flow. The movement of the particles is computed when the integration of the momentum equation for that time step is completed.

First an integer number l and n pairs (x_{0n}, z_{0n}) are chosen in the x-z-plane of the two-dimensional numerical model which will be the starting points of the streaklines. n is the index of a streakline to be displayed and l indicates the number of time steps passed since the start of the numerical model. The starting points need not to be identical to gridpoints $x_{i,j}$, $z_{i,j}$ of the numerical model.

In step 1 the first particles of the streaklines will be inserted at $(x_{n,1}(t_{l+1}), z_{n,1}(t_{l+1})) = (x_{0n}, z_{0n})$.

In step 2 a first order advection scheme is used based on a Taylor series expansion, truncated after the first order-term

$$x_{n,k}(t_{m+1}) = x_{n,k}(t_m) + \Delta t \dot{x}_{n,k}(t_m)$$
$$z_{n,k}(t_{m+1}) = z_{n,k}(t_m) + \Delta t \dot{z}_{n,k}(t_m) .$$

Here Δt is the time step of the numerical model, m is the number of the time step just completed for the momentum equations, and k is the index of a particle within one streakline $(k \leqslant m - l)$.

This method is a one step forward integration method where the integration error can grow from step to step. Let $|\delta x_{n,k}(t_m)|$ be the absolute value of the error after the m-th time step, then there is an upper bound for the error after the next time step, i.e.

$$|\delta x_{n,k}(t_{m+1})| \leqslant (1 + L \cdot h) \cdot |\delta x_{n,k}(t_m)|$$

(see, e.g., Zurmühl, 1957, p. 369ff). In our case the stepwidth h is equal to the time step Δt and the Lipschitz constant L for differentiable functions can be estimated by the largest of the absolute values of the elements of the Jacobian

$$\begin{pmatrix} \frac{\partial u}{\partial x} & \frac{\partial u}{\partial z} \\ \frac{\partial w}{\partial x} & \frac{\partial w}{\partial z} \end{pmatrix} .$$

The growth of the error of the advection scheme is negligible if $L \cdot h \ll 1$. For practical problems values between 0.1 and 0.2 are often chosen. In our case both L and h are given from the numerical flow simulation model. So we have to check *a posteriori* if $L \cdot h$ was small enough.

The velocities $\dot{x}$ and $\dot{z}$ are found by interpolation from the surrounding four gridpoint values of the mean velocity fields $u_{i,j}$ and $w_{i,j}$:

$$\dot{x}_{n,k}(t_m) = u(x_{n,k}(t_m), z_{n,k}(t_m)) = \sum_{i=i_1}^{i_2}\sum_{j=j_1}^{j_2} u_{i,j} L_i(x_{n,k}(t_m)) L_j(z_{n,k}(t_m))$$

$$\dot{z}_{n,k}(t_m) = w(x_{n,k}(t_m), z_{n,k}(t_m)) = \sum_{i=i_1}^{i_2}\sum_{j=j_1}^{j_2} w_{i,j} L_i(x_{n,k}(t_m)) L_j(z_{n,k}(t_m)) .$$

The L_i and L_j are found from

$$L_{i_1} = \frac{(x_{i_2,j} - x_{n,k}(t_m))}{(x_{i_2,j} - x_{i_1,j})}$$

$$L_{i_2} = \frac{(x_{i_1,j} - x_{n,k}(t_m))}{(x_{i_1,j} - x_{i_2,j})}$$

$$L_{j_1} = \frac{(z_{i,j_2} - z_{n,k}(t_m))}{(z_{i,j_2} - z_{i,j_1})}$$

$$L_{j_2} = \frac{(z_{i,j_1} - z_{n,k}(t_m))}{(z_{i,j_1} - z_{i,j_2})} .$$

The indices of the four gridpoints for the interpolation always obey the following relations with $i_2 = i_1 + 1$ and $j_2 = j_1 + 1$:

$$x_{i_1,j} \leqslant x_{n,k}(t_m) \leqslant x_{i_2,j}$$
$$z_{i,j_1} \leqslant z_{n,k}(t_m) = z_{i,j_2} .$$

In step 3 new particles are added to each streakline at the old origin at $(x_{n,k}(t_{l+k}), z_{n,k}(t_{l+k})) = (x_{0n}, z_{0n})$ with $k \geqslant 2$.

Step 4 is to repeat from step 2 for all n and for all k.

In order to keep the additional storage requirements on the computer at a reasonable level the number of different streaklines was set to 10 ($n = 1, \ldots, 10$) and each particle within one streakline was only followed for 500 time steps ($k = 1, \ldots, 500$) and then discarded, so the maximum number of particles to be advected in step 2 is 5000. In most of the numerical experiments this number was sufficient for the particles to reach the outflow boundary of the computing domain. In cases of stationary eddies this means that the center of the eddy starts to become clear after 500 time steps.

As the particles are only advected by the mean wind these computations should not be compared to numerical dispersion simulations.

Figure 1 is an example for the principle features of a streakline plot. It is a magnification taken from the lower left corner of the upper right figure in figure 5. For the physical background see below. The tickmarks at the horizontal axis indicate the horizontal distance of the gridpoints of the numerical model. As the vertical griddistance is variable and depending on the orography (see Part 3), a linear scale in meters is given on the vertical axis.

The chosen origins of the 10 streaklines $(x_{01}, z_{01}), \ldots, (x_{010}, z_{010})$ are near the left edge of the frame. The flow is coming from the left. In order to distinguish between different streaklines in areas of more complex motion small numbers have been used as symbols to mark the positions of the particles of the streaklines starting from « 0 » for the lowest streakline to « 9 » for the uppermost one. Every tenth particle within one streakline has been marked differently in order to indicate equal travel times from the origin. A « 1 », plotted slightly larger, indicates a particle that has been released 10 times steps ago, a « 2 » indicates a particle that has been released 20 time steps ago, and so forth. Linking these symbols by dashed lines produces phase lines in the flow. As the time step has been 3 s for this example, phase lines for 30, 60, 90, ... s travel time are displayed in figure 1.

The figure shows a jet-like flow (the highest velocity is with the streakline indicated by « 6 », the distance between two particles within one streakline is proportional to the flow velocity) and eddies forming in the lower shear flow. The lower five streaklines (marked « 0 » to « 4 ») are involved in the eddy to the right. A second eddy starts to form further left.

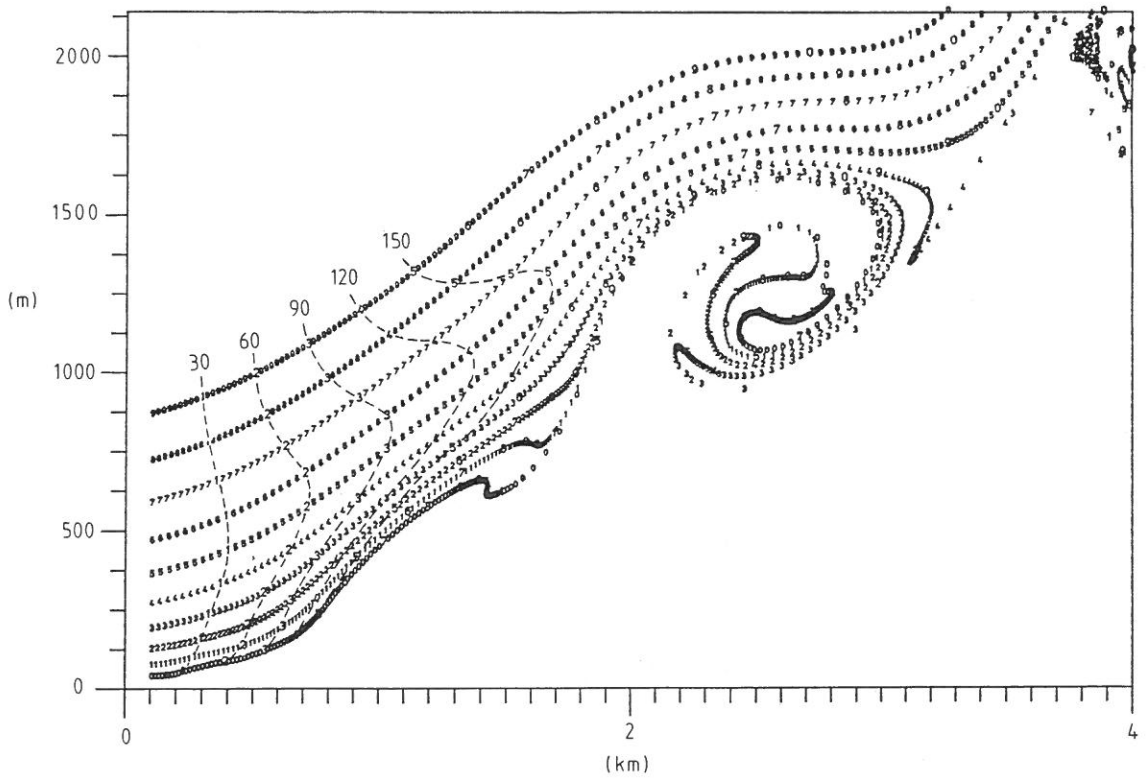

Figure 1

Example of a streakline plot. Small symbols « 0 » to « 9 » mark the ten different streaklines. Slightly larger symbols « 1 » to « 0 » at each tenth position within each streakline mark equal travel times from the origin near the left edge. Numbers at dashed lines give travel times in seconds.

As the number of streaklines is limited, only part of the flow can be made visible. The position of the streakline origins must be shifted to visualize different flow areas.

2.2. Material elements

Skipping step 3 in the production of the streaklines and only once inserting more than one particle for each streakline at a certain instant in the flow leads to the visualization of the advection of material elements in the flow. An example is given in figure 2. Here is shown how a material element is distorted when passing over a hill. In the upper figure the mean slope of the hill is 0.1, in the lower figure the mean slope is 0.4 leading to flow separation. The meaning of the tickmarks at the axes is like in figure 1.

In this figure the material element is shown for three different time steps each. In the upper figure the element is plotted 1, 6, and 17 min after the insertion, in the lower figure it is plotted 1, 8, and 17 min after the insertion. The elements in both pictures were started between the third and seventh tickmark from the left edge. The elements are made up by ten material lines (initially horizontal) consisting out of 85 particles each which are connected by (initially vertical) phase lines 10 particle positions apart each. The material lines are advected by the flow and the phase lines are then drawn to link the respective particles in the different material lines. Unlike figure 1 the material lines are not marked by different symbols but a curve has been plotted through the 85 particle positions for each line.

The two pictures in figure 2 show the different types of flow over flat and steep hills under neutral stratification. After passing the flat hill the material element is in the same height above ground again as it was inserted. The element is distorted only by the boundary layer wind shear. After passing the steep hill the material element cannot return to its original height immediatly due to the flow separation. Non-linear flow features have become important in the second case.

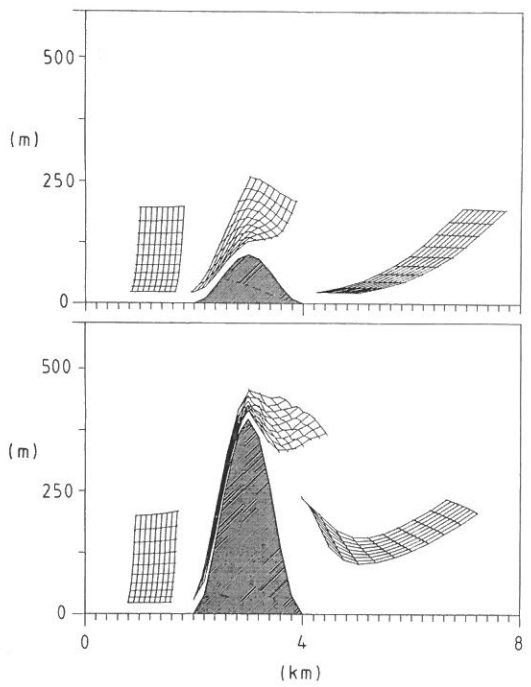

Figure 2
Advection of a material element over a flat hill with aspect ratio 0.1 *(top) and over a steep hill with aspect ratio* 0.4 *(bottom). For details see text.*

3. DESIGN OF THE NUMERICAL EXPERIMENT

The two-dimensional version of the mesoscale numerical model KAMM (Karlsruhe Atmospheric Mesoscale Model) developed at the Institut für Meteorologie und Klimaforschung has been used for this study. The model is a prognostic, nonhydrostatic, primitive-equation gridpoint-model with a constant horizontal and a variable vertical gridwidth (Dorwarth, 1985 ; Emeis, 1987). In the following examples vertical gridwidth varies from 14 m in the lower boundary-layer to some hundred meters in the upper troposphere and horizontal gridwidth is 100 m. The time-step chosen is 2 s. The number of gridpoints is 122 and 30 in the horizontal and vertical directions respectively. The height of the model domain is 8000 m.

Turbulence closure is done by a two-equation model for eddy-viscosity. There are two prognostic equations for the turbulent kinetic energy and the mixing length.

Boundary conditions are a no-slip condition at the lower boundary which is identical to the topography (the coordinate system follows topography), radiation conditions at the lateral boundaries and a damping layer at the top of the model domain.

The principal design of the numerical flow simulation which is to demonstrate the usage of streaklines is as follows.

The flow passes a step from a plateau down to flat terrain. The air over the plateau is stably stratified such that a shooting flow with a hydraulic jump further downstream results. The orographic setting determines the large-scale features of the flow. Surface roughness length is kept constant in the whole domain to 0.5 m. The geostrophic wind which describes the external forcing by a large-scale pressure gradient in the model is 8.5 m s^{-1}. Such types of flow can be found with Bora at the Adriatic coast or with severe downslope windstorms (Smith, 1985 ; Lilly, 1978 ; Clark and Peltier, 1984).

The surface temperature of the step slope and the following terrain is increased by 3 K and 1 K respectively to simulate an insolated slope and a warm daytime surface. This leads to warm bubbles rising with and downstream of the hydraulic jump. The bubbles form the smallest features in the flow. They disturb the interface between the heated surface layer downstream of the hydraulic jump and the stable layer above. These disturbances lead to the excitation of Kelvin-Helmholtz-waves at the interface. Smith and Carson (1977) have presented a conceptual picture of exchange and entrainment processes at such an interface (fig. 3).

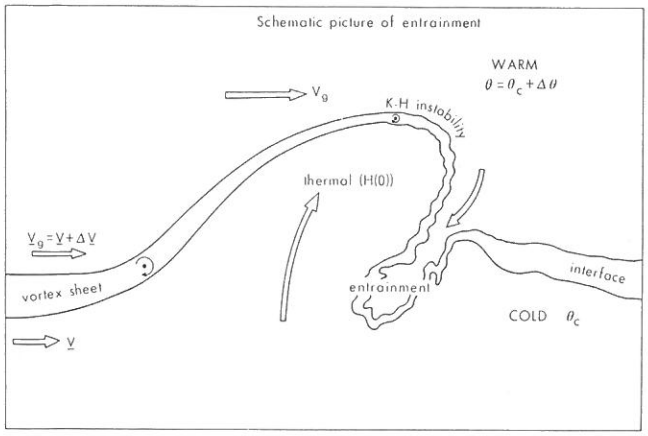

Figure 3
Conceptual picture of entrainment processes at an internal boundary-layer by Smith and Carson (1977).

This picture represents schematically some of the interacting dynamical and thermal processes which are important for the entrainment. The interfacial zone is a layer of marked (shear) vorticity. Small disturbances, e.g. by thermals cause local enhancement of vorticity which results in tongues of warm air being driven down into the (potentially) colder boundary-layer.

Kelvin-Helmholtz-waves can occur at this interface. These waves are unstable when they are shorter than a critical wavelength

$$\lambda_c = \frac{2\pi}{g} \frac{\Theta_1 \Theta_2}{(\Theta_1 + \Theta_2)} \frac{(\Delta u)^2}{\Delta\Theta}.$$

The critical wavelength is growing with increasing shear and decreasing with increasing temperature differences. So, a pure temperature discontinuity is always stable and a pure shear discontinuity is always unstable. Some typical values for λ_c are given in table 1. The equation for λ_c is deduced from the equation for the phase velocity of waves at a density and wind discontinuity. The equation is strictly valid only for homogeneous media on both side of the discontinuity (see e.g., Pichler, 1984, p. 274ff). In the numerical model a shear zone forms instead of a real discontinuity and the stratification above and below the shear zone is not perfectly neutral.

Table 1
Critical wavelengths for Kelvin-Helmholtz waves. Given are wind and potential temperature differences across the internal boundary layer. $\Delta u = u_2 - u_1$, $\Delta\Theta = \Theta_2 - \Theta_1$.

Δu = 5 m s^{-1}	$\Delta\Theta$ = 5 K	Θ_1 = 290 K	Θ_2 = 295 K	$\lambda_c \sim 0.5$ km
Δu = 10 m s^{-1}	$\Delta\Theta$ = 5 K	Θ_1 = 290 K	Θ_2 = 295 K	$\lambda_c \sim 2$ km
Δu = 10 m s^{-1}	$\Delta\Theta$ = 1 K	Θ_1 = 294 K	Θ_2 = 295 K	$\lambda_c \sim 10$ km

4. RESULTS

Figures 4 and 5 show two flow simulations with different ambient stable temperature stratifications (0.005 K m^{-1} and 0.003 K m^{-1}) leading to stable and unstable Kelvin-Helmholtz-waves (K-H-waves). Downstream of the hydraulic jump an internal boundary forms (see also fig. 6). For the case in figure 4 the wind difference across this boundary layer is of order 10 m s^{-1} whereas the temperature difference is about 5 K. Following table 1 a critical wavelength of about 2 km can be expected. For the case in figure 5 the wind difference is again about 10 m s^{-1} but the temperature difference is only about 3 K so that a critical wavelength for the K-H-waves of about 4 km can be expected.

In both figures 4 and 5 the streaklines are started 1 km downstream of the step. Clearly three interacting scales of motion can be detected. The largest scale is formed by the hydraulic jump. At the interface between the stable layer above and the boundary layer below, K-H-waves with a wavelength of about 3 km move downstream. These waves are triggered by

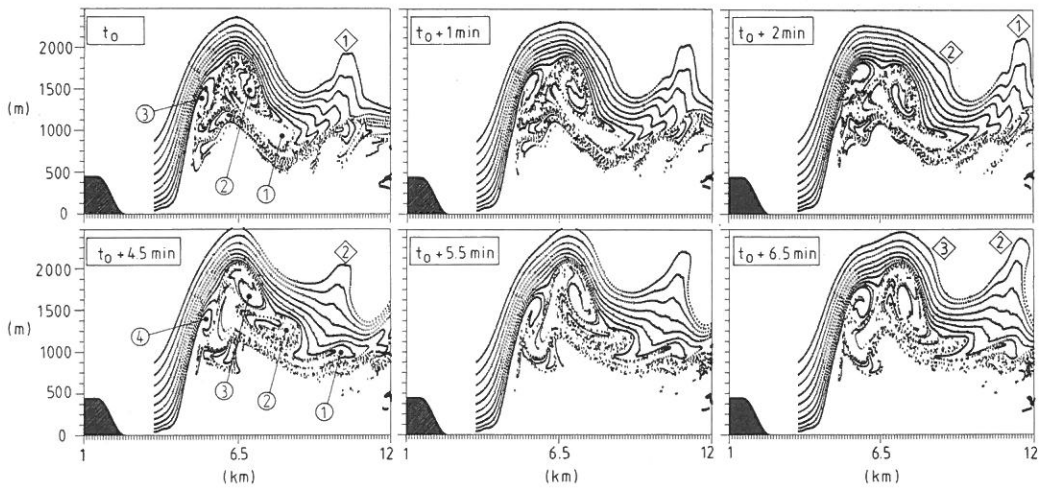

Figure 4
Times series of streakline plots for stable Kelvin-Helmholtz-waves (critical wavelength is about 2000 m*). Eddies are marked by numbers* 1 *to* 4 *in circles,* K-H-*waves by numbers* 1 *to* 3 *in rhomboids. The step is seen near the left edge. See text for further details.*

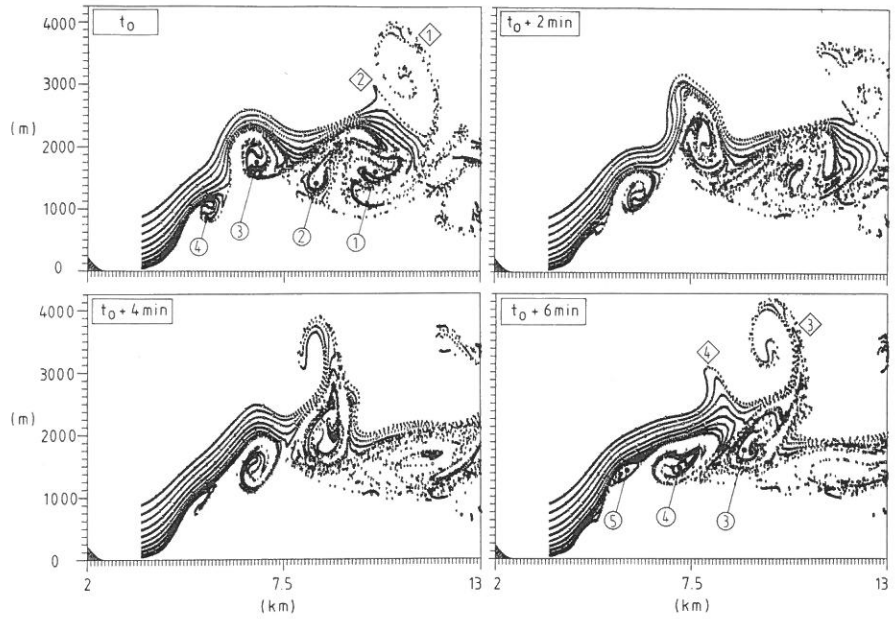

Figure 5
As figure 4 but for unstable Kelvin-Helmholtz-waves (critical wavelength is about 4000 m). The domain plotted is shifted 1 km to the right compared to figure 4.

disturbances with a typical scale of about 1 km coming from the unstable region below.

The *a posteriori* check of the stability criterion $L \cdot h$ for the integration of the streaklines shows that with the exception of the vertical wind shear in the lowest 200 m above ground the maximum of the error growth $L \cdot h$ in the whole domain is always between 0.15 and 0.18. The potential instability in the lowest 200 m is of no importance for the streaklines in figures 4 and 5 as all eddies and waves displayed are at least 1000 m above ground.

In figure 4 the wavelength of the K-H-waves is longer than the critical wavelength and so the waves remain stable. The disturbances which form at the lower side of the internal boundary layer are marked by the numbers in circles, the K-H-waves excited by them by numbers in rhomboids. From the sequence of the streakline plots it can be seen that the flow patterns repeat every 4 1/2 min.

As the waves are stable no air from above can enter the layer below the internal boundary layer. This is well documented by the streaklines. The upper lines are continuous, they indicate a quasi laminar flow, and only particles from the lower streaklines have entered the eddies below the internal boundary layer.

In figure 5 the wavelength of the K-H-waves is smaller than the critical wavelength and so the waves are unstable. K-H-wave number 1 (number in rhomboid) has already broken (upper left frame) and wave number 2 is included in the breaking wave number 1. In the sequence of the streakline plots wave number 3 forms and then breaks, too (lower frames). Wave number 4 is again included in the preceding breaking wave. After about 7 min the flow pattern is repeating.

Here the streaklines clearly show the strong interaction and interchange between the two layers above and below. On the upstream side of the breaking wave particles are ejected high up into the stable layer. On the downstream side particles from the upper streaklines are included in the eddies below. This depicts the exchange and entrainment processes in the conceptual picture of Smith and Carson (1977). On the original plots the different symbols marking the particles from different streaklines can be dis-

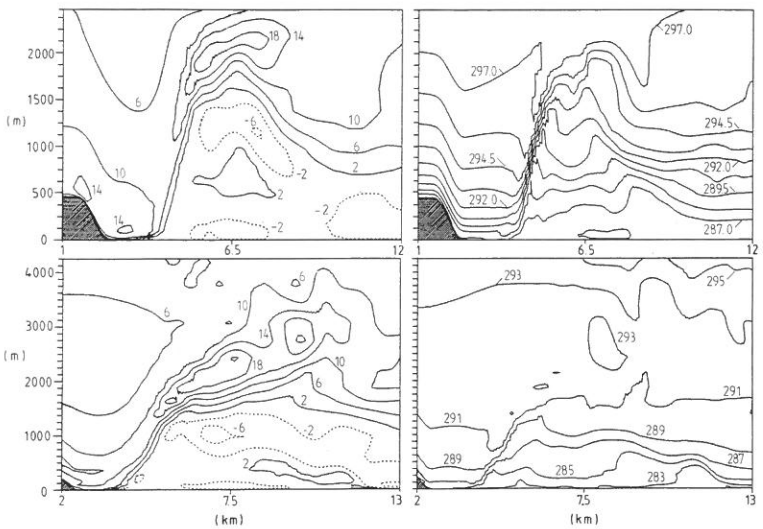

Figure 6
Horizontal wind (left) and potential temperature (right) for the cases shown in the lower right frames of figures 4 (top) and 5 (bottom). Isoline increments are 4 m s^{-1} for the wind fields and 1.25 K (top) and 2 K (bottom) for the temperature fields.

tinguished (see fig. 1) but for the sake of showing complete flow structures the different symbols are unfortunately not to be distinguished clearly here.

Figure 6 shows contour plots for the horizontal wind component and potential temperature for both cases for the lower right frames in figures 4 and 5 each. The wind and temperature shear zones marking the internal boundary layer are obvious, but the positions of the eddies below and the waves above the shear zone could only be fixed with reference to the vertical wind distribution (not plotted here). The shape of the eddies and the breaking waves can merely be detected from the contour plots. The comparison of figures 4 and 5 with figure 6 shows that streakline plots and contour plots give different kinds of information which are both necessary. Whereas contour plots show the overall features of the flow in the whole domain streakline plots are a convenient tool to visualize more small scale, instationary structures in limited parts of the flow domain.

Figure 7 shows the horizontally averaged wind and potential temperature profiles and the gridscale vertical turbulent momentum fluxes downstream of the hydraulic jump for the two cases presented in figures 4 (full lines, index A) and 5 (broken lines, index B). Clearly the more stable stratification of the first case can be seen. Figure 4 has shown that the height of the interface between the boundary-layer and the stable layer above is between 1000 m and 2000 m. Just above this interface the wind speed is maximum. Through the interface there is a downward gridscale momentum flux of about 1 $m^2 s^{-2}$. The subgridscale momentum flux (not plotted here) which is parameterized in the numerical model is less than 10 % of the gridscale momentum flux. Above the wind speed maximum there is upward gridscale momentum flux. The gridscale momentum flux is nearly always directed down the gradient of the mean wind speed.

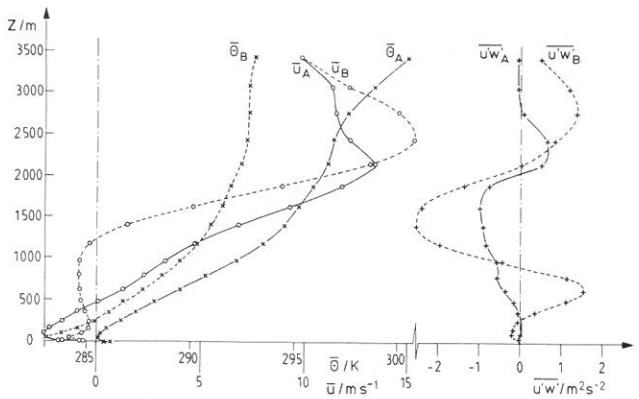

Figure 7

Horizontally averaged wind and potential temperature profiles and the gridscale vertical turbulent momentum fluxes downstream of the hydraulic jump. Full lines correspond to the case in figure 4 (index A) and broken lines to the case in figure 5 (index B).

In the case of unstable K-H-waves (fig. 5) the gridscale vertical momentum fluxes are two to three times larger than for the stable K-H-waves. In this case the vertical exchange processes are so strong that a nearly neutral layer forms between 2000 m and 3000 m height.

5. CONCLUSIONS

Plots of streaklines and material elements have been presented as a tool for the analysis of atmospheric flows computed with numerical models. Just one additional transport equation for a passive tracer substance is needed in the model for this purpose.

Streaklines have proved to be a convenient tool to visualize instationary, smaller-scale flow patterns. The formation, growth, and decay of coherent structures as eddies in a shear flow was documented. The breaking of waves was displayed. This method is the analogy to continuous injection of smoke or dye in air or water flow in wind and water tunnels.

The usage of different symbols for different streaklines allowed to follow exchange processes between different flow regions. The origin of each particle is known.

With small changes to the insertion of particles and to the final plotting routine also the distortion of material elements in a flow can be made visible. This is in analogy to discontinuous injection of tracer substances in a flow in wind or water tunnel experiments.

Comparison of streakline plots to contour plots demonstrated that instationary processes such as small eddies and breaking waves can hardly be detected from contour plots.

On the other hand contour and streamline plots show the overall flow features in the whole domain whereas streaklines and material elements can only be used to visualize limited parts of the flow. So both types of graphical presentation are necessary for a full discussion of results of numerical models.

Two numerical experiments were presented in this paper. The passing of material elements over a hill showed different types of flow over flat and steep hills. The distortion of the material elements during their travelling gives hints whether linear theories are applicable or non-linear effects become important.

The streaklines were used to show scale interactions in a flow behind a step. The resultant features fit well into a conceptual picture of exchange and entrainment processes by Smith and Carson (1977).

Three different interacting scales have been shown. Downstream of the large-scale lee wave (or here : hydraulic jump) the interaction between small-scale disturbances (eddies) and Kelvin-Helmholtz-waves was made visible.

Gridscale vertical momentum fluxes have been computed from the mesoscale model. In the case studies presented they are ten times larger than the subgridscale (turbulent) momentum fluxes which are parameterized in the numerical model. For the unstable K-H-waves the gridscale vertical momentum fluxes were two to three times larger than for the stable K-H-waves.

Streakline plots should become a more frequent tool in analyzing results of numerical atmospheric flow simulations.

Acknowledgements

This study is part of the work done in the Sonderforschungsbereich 210 at Karlsruhe University funded by the Deutsche Forschungsgemeinschaft. My thanks are to Prof. Fiedler and all co-workers at the Institut für Meteorologie und Klimaforschung in Karlsruhe who maintain and further develop the numerical model.

REFERENCES

Clark, T. L., and W. R. Peltier, Critical level reflection and the resonant growth of nonlinear mountain waves, *J. Atmos. Sci.*, **41,** 3122-3134, 1984.

Davis, R. W., and E. F. Moore, A numerical study of vortex shedding from rectangles, *J. Fluid Mech.*, **116,** 475-506, 1982.

Dorwarth, G., Numerische Berechnung des Druckwiderstands typischer Geländeformen, *Dissertation Univ. Karlsruhe, Berichte des Sonderforschungsbereichs SFB210,* SFB210/T/20, 1985.

Eaton, B. E., Analysis of laminar vortex shedding behind a circular cylinder by computer-aided flow visualization, *J. Fluid Mech.*, **180,** 117-145, 1987.

Emeis, S., Pressure drag and effective roughness length with neutral stratification, *Bound.-Layer Meteorol.*, **39,** 379-401, 1987.

Lilly, D. K., A severe downslope windstorm and aircraft turbulence event induced by a mountain wave, *J. Atmos. Sci.*, **35,** 59-77, 1978.

Perry, A. E., M. S. Chong, and T. T. Lim, The vortex-shedding process behind two-dimensional bluff bodies, *J. Fluid Mech.*, **116,** 77-90, 1982.

Pichler, H., *Dynamik der Atmosphäre,* B.I. Wissenschaftsverlag, Wien, 456 p., 1984.

Smith, F. B., and D. J. Carson, Some thoughts on the specification of the boundary-layer relevant to numerical modelling, *Bound.-Layer Meteorol.*, **12,** 307-330, 1977.

Smith, R. B., On severe downslope winds, *J. Atmos. Sci.*, **42,** 2597-2603, 1985.

Zurmühl, R., *Praktische Mathematik für Ingenieure und Physiker,* Springer Verlag, Berlin/Göttingen/Heidelberg, 524 p., 1957.